Performance Analysis of Mm-Wave Wearable Antennas for Visually Impaired Aid

A. Flórez Berdasco[1], J. Laviada[1], M. E. deCos Gómez[1], F. Las-Heras Andrés[1]
[1] TSC Electrical Engineering Dept., Gijón, Spain, florezalicia@uniovi.es

***Abstract*—The evaluation of the performance of several wearable antennas for helping visually impaired people by means of radar technology, is presented. The antennas have been designed *ad hoc* for this application in the 24.05 to 24.25 GHz unlicensed frequency band. Based on Synthetic Aperture Radar (SAR) techniques, a simulation for each antenna has been performed in short distance to obtain an electromagnetic image of the target. In order to assess the quality of the electromagnetic images, an error metric has been applied, so that the behavior of the antennas is analyzed and compared for this application.**

Index Terms—Synthetic Aperture Radar (SAR), Electronic travel Aid (ETA), mmWave radar, mmWave imaging, Imaging.

I. INTRODUCTION

Radar systems operate by transmitting a signal into the space and detect the echo signal reflected by the targets. Comparing the received echo signal with the transmitted one, the distance, position and speed of targets can be determined. During the last years, this technology, conveniently adapted to the mmWave band to benefit from compactness and high-resolution capabilities, has been included by the automotive industry in advanced driver-assistance systems (ADAS) and, therefore, this kind of radars have been extensively developed reducing their cost. Besides that, radar technology can detect visible and hidden objects, and it can work in darkness, haze, and bad weather conditions such as in fog, dust, or smoke. Its best attribute is the capacity to calculate the position and the speed of objects with high accuracy and in all environment and weather conditions [1].

Nowadays, it is estimated that 1.3 billion people worldwide suffer from some kind of visual impairment [2]. A part of them, need a support system in their daily life. The most extended ones are the white cane, which it is not enough for safe mobility, since it does not prevent from upper body collisions, and the guide dog, which must be trained for this task. Nevertheless, they do not fully allow autonomy [3]-[4]. For this reason, during the last years a great number of electronic travel aid (ETA) systems have been proposed. Ultrasound sensing have been widely employed for this purpose, due to its low cost. Nevertheless, its wide radiation pattern difficulties detecting narrow openings and flat surfaces [5]-[6]. Optical based technologies (e.g., cameras), have been presented as ETA, but in low visibility conditions, they do not operate [7]. These are some examples among other solutions. However, these proposed systems are not enough for safety mobility since they have limitations on accuracy or scope.

In the absence of a robust technology for ETA application, the mmWave radar-based systems have been developed in recent years, due to the mentioned advantages of this technology in terms of scope, accuracy, and operation capacity in all environmental conditions. For example, in [8], a portable vector network analyzer is used for testing the detection either indoor or outdoor scenarios. The system was able to detect more than one obstacle. A frequency-modulated continuous wave radar-based system is presented in [9], which operates at the center frequency of 80 GHz. The radar was situated at the head of a blind person. This sensor scans the surrounding of the user and detects the position of obstacles up to 5 m. The combination of a mmWave radar and an RGB-depth sensor is explored in [10]. The position and velocity information are provided by the mmWave radar, while the depth of the obstacles is supplied by the RGB-depth sensor. It is demonstrated that the combination improves the detection results. In addition, the use of natural movement to create a synthetic aperture and, therefore, improving the resolution has also been proposed in [11]. Nevertheless, in order to ease the use of these systems, they should be wearable, which typically requires the use of antennas that can be easily embedded in clothing. However, the impact of the radiation pattern of the antennas, for this application, in the electromagnetic images have not been typically considered, though it has been recently received some attention [12], [13].

This work analyzes the effect of nonideal radiators in this kind of electromagnetic images. The study is done by considering the radiation pattern for a set of antennas, designed specifically for this application.

The paper is organized as follows: first the main concerns about the imaging algorithm, the set of antennas and the error metric applied to assess the quality of the antennas is explained. Then, the results are exposed and analyzed. Finally, conclusions are drawn.

II. OBSTACLE DETECTION FOR SHORT RANGE APPLICATION

A. Electromagnetic Image Algorithm

As previously discussed, high resolution imaging can be achieved by considering the natural movement when a radar system is attached to the body [11]. In this case, the images can be computed by means of a flexible sum-and-delay algorithm for monostatic acquisition system, according to

$$\rho(\vec{r}) = \sum_{m=1}^{M} \sum_{n=1}^{N} S_{11}(m,n) \cdot e^{jk_m 2|\vec{r}-\vec{r}_n|}, \qquad (1)$$

S_{11} stands for the acquired data, $\vec{r}$ refers to the pixel where reflectivity will be computed, $\vec{r}_n$ represents the *n-th* measured position and k_m indicates the wavenumber at the m-frequency. *M* refers to the number of frequencies, while *N* to the acquisition points. Fig. 1 shows the schematic of the sum-and-delay algorithm.

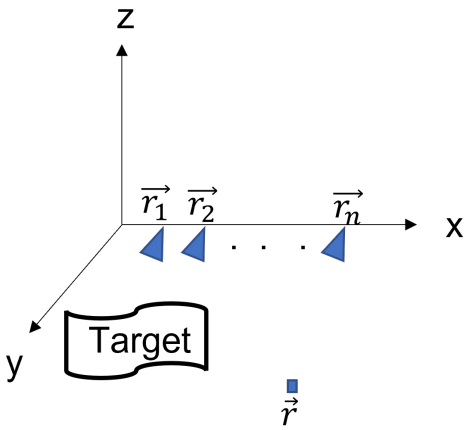

Fig. 1. Schematic of the synthetic aperture radar (SAR) imaging algorithm.

It is necessary to remark that the algorithm (1) assumes that the waves are created for all frequencies at the same position, generating a perfect spherical wavefront without dispersive behavior along frequency. As it will be shown later, if those characteristics are not met, relevant artifacts will take place.

B. Antennas

A set of wearable antennas has been designed *ad hoc* for this application. All of them operate in the unlicensed frequency band 24.05 to 24.25 GHz, where final application can be implemented. RO3003 (whose electrical permittivity is ε_r=3, loss tangent tanδ=0.0013 with a thickness of *h*=0.762mm) has been selected as the substrate of the antennas.

The details about the antenna design can be found in [14]-[15]. Antennas with an omnidirectional radiation pattern are compared with a high-gain antenna. On the one hand, the low-directivity antennas are a patch (see Fig. *2*a), a 2-elements array (referred to as *Basic Array*, see Fig. *2*b), and the combination of this array with a High Impedance Surface (HIS) metasurface to improve its radiation properties. The HIS metasurface has been arranged between the patches (referred to as *Wall*), with the aim of reducing the coupling between them (see Fig. *2*c), surrounding the patches (referred to as *Row*) in order to reduce the potential surface waves (see Fig. *2*d) and including a new row of unit-cells (referred to as *2Row*) in front of the patches to study their behavior (see Fig. *2*e). On the other hand, a modified Dolph-Chebyshev distribution series end-feed 10 elements array antenna (referred to as *DC*, see Fig. *2*f), with high directivity in one of its main planes, has been considered in order to compare the results between directive an omnidirectional radiation pattern is this kind of application. Fig. *2* shows the antennas.

TABLE 1 summarizes the radiation properties of the antennas at the center of the intended frequency band (24.15 GHz), according to the simulations performed in HFSS.

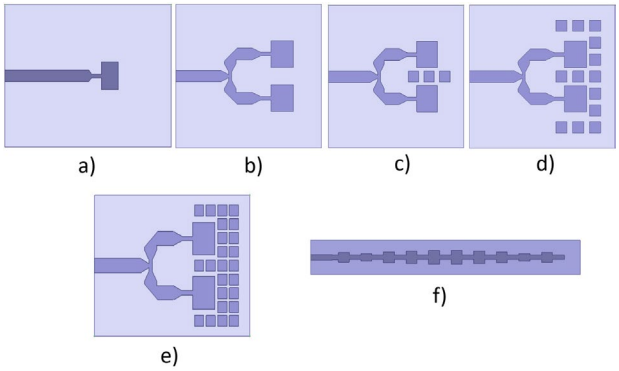

Fig. 2. Antennas under test: a) Patch, b) Basic Array, c) Wall, d) Row, e) 2Row and f) DC.

TABLE 1 RADIATION PROPERTIES OF THE ANTENNAS UNDER TEST (24.15 GHZ): GAIN (G), DIRECTIVITY (D), EFFICIENCY (P) AND FRONT-TO-BACK RATIO (FTBR)

Antennas	G [dB]	D [dB]	η [%]	FTBR [dB]
Patch	6.8	6.8	100	20.2
Basic Array	7.3	7.4	98	19
Wall	8	8	100	24.8
Row	7.9	7.9	100	36.7
2Row	9.2	9.2	100	17
DC	15.5	15.6	98	23.9

C. Error Metric

In order to quantitatively evaluate and compared the electromagnetic images obtained with each antenna, the target to clutter ratio (TCR) error metric is used in this work. The TCR is commonly used to evaluate the quality of SAR images [12]. This error metric determines the amount of energy around the target. It is calculated according to

$$TCR = 10log_{10}\left(\frac{N_c \Sigma_{(x,y)\in A_t}|\rho(x,y)|^2}{N_t \Sigma_{(x,y)\in A_c}|\rho(x,y)|^2}\right), \quad (3)$$

ρ refers to the reflectivity, A_t represents the area inside the target and A_c the area outside it. N_t and N_c stand for the number of pixels inside and outside the target.

In order to evaluate the previous expressions, the contour of the object is used as the mask that delimits the pixels inside and outside the target.

III. RESULTS

With the aim of evaluating the performance of the antennas for a radar application to avoid collisions at short distance, electromagnetic images of a close object have been obtained by simulation to assess the target detection.

For this purpose, a pure monostatic system has been simulated by means of ideal transmitting and receiving antennas in Feko, with the far-field radiation pattern obtained previously from HFSS, has been moved over a plane of 20x20cm. In order to thoroughly analyze the impact of the antenna radiation pattern for electromagnetic imaging and highlight the corresponding defects, a two-dimensional scan has been carried out instead of the one-dimensional proposed in [12]. A pair of scissors has been used as the target as it provides a demanding complex shape when obtaining these images (see Fig. 3). The sampling step has been set to $\frac{\lambda}{2}$ (λ calculated at the highest frequency of the considered bandwidth) along both directions in the XY plane.

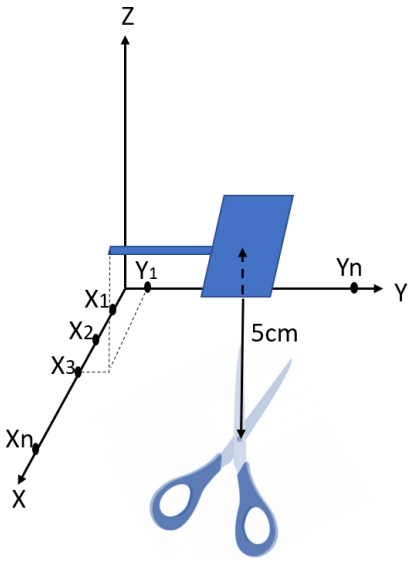

Fig. 3. Simulation setup

Likewise, it is necessary to remark that, even if the electromagnetic images are obtained in the near-field (5 cm from the target), in order to keep an affordable computational cost some approximations are done. In particular, the radiation pattern of the antennas used in this simulation is the far-field.

Electromagnetic images have been obtained according to (1) for each antenna at the desired frequency band. Fig. 4 shows the electromagnetic images at XY plane when the antenna is placed at 5 cm from the scissors. As it can be seen, the scissors can be identified in all cases, though artifacts and displacement can be observed. In order to quantify the results in terms of the TCR, an investigation domain, coinciding with the contour of the scissors, has been established, as it can be seen in color red in the electromagnetic images shown in Fig. 4. The results are presented in TABLE 2. As it can be seen in Fig. 4, there are a lot of artifacts around the target. Most of them are produced due to the reduced available bandwidth of the band, which avoids the use of more frequencies to cancel out those artifacts. Nevertheless, the target is identified in all cases. The TCR results are similar for the 2-elements array (Basic Array, Wall, Row) except for the 2Row antenna, which shows a better behavior. However, the patch antenna and the DC one exhibit worse TCR. In the case of the patch antenna differences are attributable to the observed vertical offset, which is expected to be due to phase changes along the beamwidth of the radiation pattern of the antenna, whereas the DC antenna exhibits a directive radiation pattern, so that it is expected that it does not illuminate the target from all acquisition data positions, limiting their effective aperture size [13].

It is also relevant to note that, though not shown here, when considering multiple frequencies, the artefacts, which are mostly frequency dependent, cancelled out, enabling a higher quality figure (i.e., if the system could extend beyond the range 24.04-24.25 GHz). However, the offset is preserved.

TABLE 2 ERROR METRIC RESULTS FOR EACH ANTENNA

Antennas	TCR (dB)
Patch	1.2
Basic Array	4.0
Wall	4.8
Row	4.8
2Row	5.1
DC	3.6

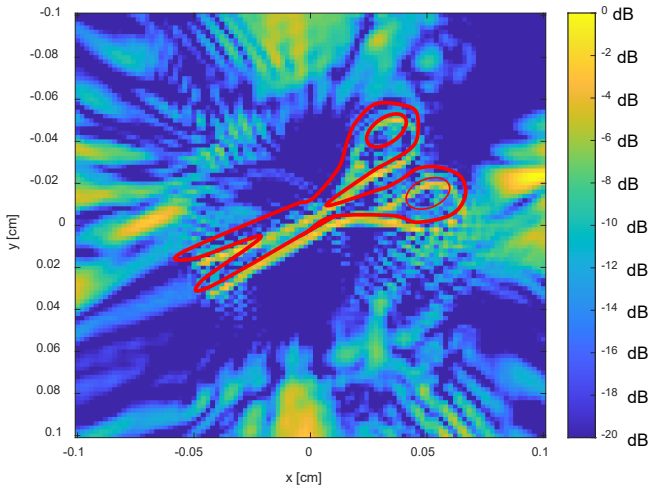

a)

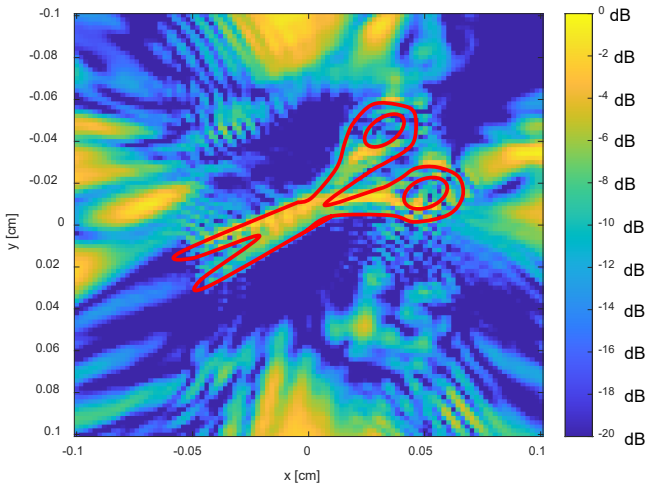

b)

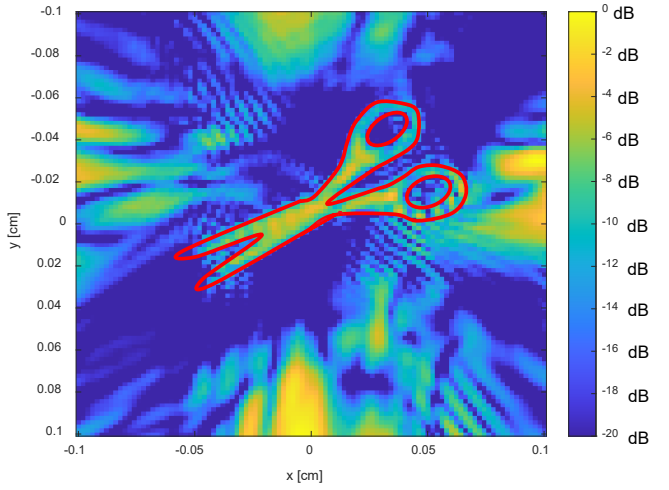

c)

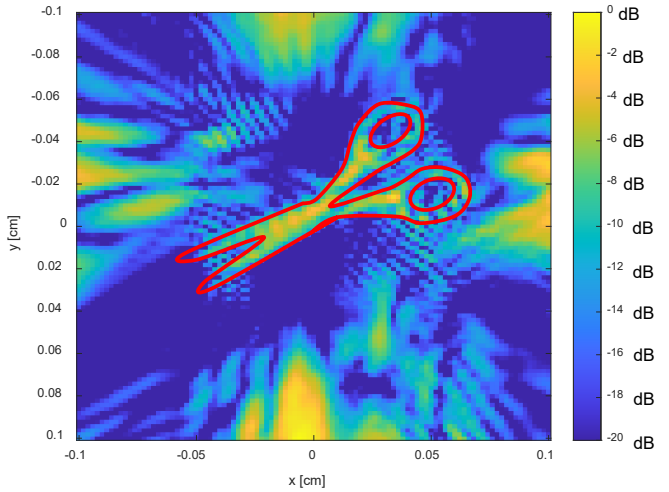

a)

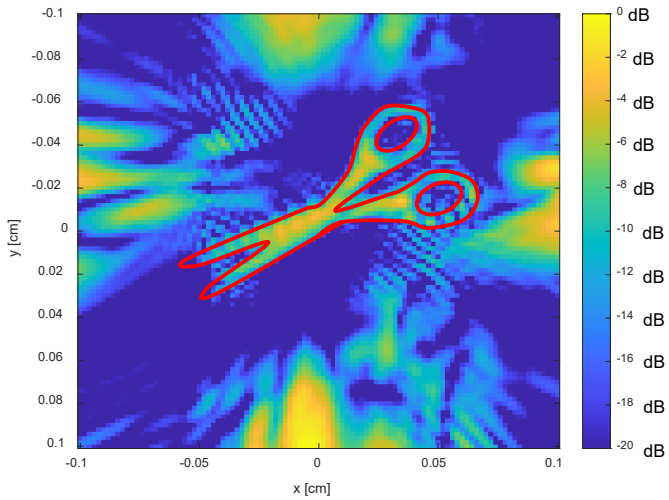

b)

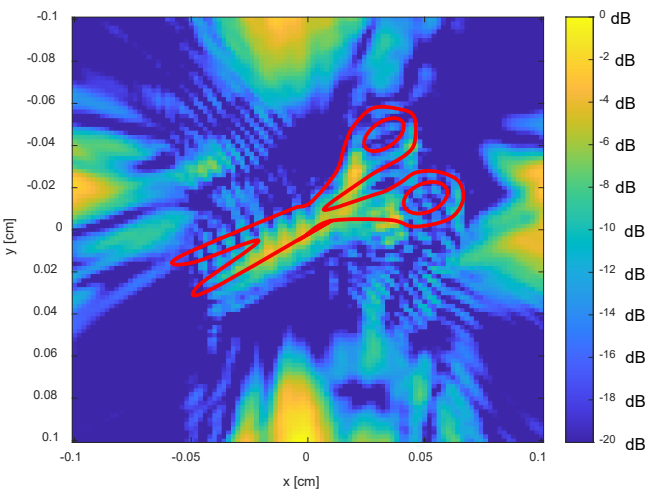

c)

Fig. 4. Electromagnetic images obtained with each antenna at plane XY. a) Patch, b) Basic Array, c) Wall, d) Row, e) 2 Rows and f) DC.

IV. CONCLUSIONS

The performance analysis of several antennas, designed *ad hoc* for a mmWave radar application to help visually impaired people has been done.

Electromagnetic images have been obtained from simulated radiation patterns at the 24 GHz unlicensed frequency band.

The comparison of nonideal performance of the antennas has been carried out throughout an error metric (TCR) applied to the electromagnetic images. From the TCR results, it follows those antennas with low directivity, behave better for near-field detection, so that omnidirectional radiation patterns are preferred. However, even for simple antennas, a careful inspection of those radiation patterns should be considered in order to avoid unwanted offsets that could degrade the quality of the images. Furthermore, the use of narrow frequency band highlights that any defect in the radiation patter highly amplifies artifacts in the image as the frequency averaging is only moderated.

ACKNOWLEDGMENT

Funded by the Ministerio de Ciencia e Innovación of Spain under the FPI Grant MCIU-20-PRE2019-089912 and project META-IMAGER PID2021-122697OB-I00, and by Gobierno del Principado de Asturias under project AYUD-2021-51706.

REFERENCES

[1] I. M. Skolnik, Introduction to RADAR Systems, New York, NY, USA: McGraw-Hill, 1980.

[2] Online: https://www.who.int/es/news-room/fact-sheets/detail/blindness-and-visual-impairment

[3] L. Scalise et al., "Experimental Investigation of Electromagnetic Obstacle Detection for Visually Impaired Users: A Comparison With Ultrasonic Sensing," *IEEE Transactions on Instrumentation and Measurement*, vol. 61, no. 11, pp. 3047-3057, Nov. 2012, doi: 10.1109/TIM.2012.2202169.

[4] J. Strada, Visually Impaired: Assistive Technologies, Challenges and Coping Strategies, Nova Science Pub Inc., February 1, 2016.

[5] E. Cardillo ,A. Caddemi, “Insight on Electronic Travel Aids for Visually Impaired People: A Review on the Electromagnetic Technology,” *Electronics* 2019, *8*, 1281. https://doi.org/10.3390/electronics8111281

[6] G E. Cardillo, C. Li and A. Caddemi, “Millimeter-Wave Radar Cane: A Blind People Aid With Moving Human Recognition Capabilities,” *IEEE Journal of Electromagnetics, Rf and Microwaves in Medicine and Biology*, vol. 6, no. 2, pp. 204-211, June 2022, doi: 10.1109/JERM.2021.3117129.

[7] A. Zvironas, M. Gudauskis and D. Plikynas, “Indoor Electronic Traveling Aids for Visually Impaired: Systemic Review,” *2019 International Conference on Computational Science and Computational Intelligence (CSCI)*, 2019, pp. 936-942, doi: 10.1109/CSCI49370.2019.00178.

[8] V. Di Mattia et al., “An electromagnetic device for autonomous mobility of visually impaired people,” 2014 44th European Microwave Conference, 2014, pp. 472-475, doi: 10.1109/EuMC.2014.6986473.

[9] P. Kwiatkowski, T. Jaeschke, D. Starke, L. Piotrowsky, H. Deis and N. Pohl, “A concept study for a radar-based navigation device with sector scan antenna for visually impaired people,” 2017 First IEEE MTT-S International Microwave Bio Conference (IMBIOC), 2017, pp. 1-4, doi: 10.1109/IMBIOC.2017.7965796.

[10] N. Long, K. Wang, R. Cheng, W. Hu, K. Yang. “Unifying obstacle detection, recognition, and fusion based on millimeter wave radar and RGB-depth sensors for the visually impaired,” Rev Sci Instrum, 2019 Apr, 90(4):044102, doi: 10.1063/1.5093279. PMID: 31042998.

[11] Y. Gao, M. T. Ghasr and R. Zoughi, “Effects of translational position error on microwave synthetic aperture radar (SAR) imaging systems,” 2018 IEEE International Instrumentation and Measuremen Technology Conference (I2MTC), 2018, pp. 1-6, doi. 10.1109/I2MTC.2018.8409556.

[12] H. F. Álvarez, G. ÁLvarez-Narciandi, F. Las-Heras and J. Laviada, “System Based on Compact mmWave Radar and Natural Body Movement for Assisting Visually Impaired People,” in IEEE Access, vol. 9, pp. 125042-125051, 2021, doi: 10.1109/ACCESS.2021.3110582.

[13] Y. Gao, M. T. Ghasr and R. Zoughi, "Effects of and Compensation for Translational Position Error in Microwave Synthetic Aperture Radar Imaging Systems," IEEE Transactions on Instrumentation and Measurement, vol. 69, no. 4, pp. 1205-1212, April 2020, doi: 10.1109/TIM.2019.2910340.

[14] Y. Álvarez and F. Las-Heras, “On the use of an Equivalent Currentsbased Technique to improve Electromagnetic Imaging,” IEEE Transactions on Instrumentation and Measurement, vol. 71, pp. 1 -13, 2022, art. no. 8004113, doi: 10.1109/TIM.2022.3181926

[15] A. F. Berdasco, M. E. de Cos Gómez, H. F. Álvarez and F. L. -H. Andrés, “Array Antenna with HIS Metasurface for mmWave Imaging Applications,” 2022 16th European Conference on Antennas and Propagation (EuCAP), 2022, pp. 1-5, doi: 10.23919/EuCAP53622.2022.9769433.

[16] M. E. de Cos Gómez, H. F. Álvarez and F. L. -H. Andrés, “Millimeter Wave Antenna on Eco-friendly Substrate for Radar Applications,” 2022 16th European Conference on Antennas and Propagation (EuCAP), 2022, pp. 1-5, doi: 10.23919/EuCAP53622.2022.9769364.